ISSN 1070-3284, Russian Journal of Coordination Chemistry, 2015, Vol. 41, No. 10, pp. 688–694. © Pleiades Publishing, Ltd., 2015.
Original Russian Text © N.V. Somov, F.F. Chausov, R.M. Zakirova, I.V. Fedotova, M.A. Shumilova, V.A. Aleksandrov, V.G. Petrov, 2015, published in Koordinatsionnaya Khimiya, 2015, Vol. 41, No. 10, pp. 634–640.

Synthesis, Structure, and Properties of the Stabilized Coordination Chrome(II) Complex with Nitrilotris(methylenephosphonic) Acid $[Cr^{II}(H_2O)_3$-μ-$NH(CH_2PO_3H)_3]$

N. V. Somov[a, *], F. F. Chausov[b], R. M. Zakirova[b], I. V. Fedotova[b], M. A. Shumilova[c], V. A. Aleksandrov[c], and V. G. Petrov[c]

[a] *Nizhny Novgorod State University, pr. Gagarina 23, Nizhny Novgorod, 603600 Russia*
[b] *Udmurt State University, ul. Krasnoarmeiskaya 71, Izhevsk, 426034 Russia*
[c] *Institute of Mechanics, Ural Branch, Russian Academy of Sciences, Izhevsk, Russia*
**e-mail: somov@phys.unn.ru*

Received March 18, 2015

Abstract—The chrome(II) complex $[Cr^{II}(H_2O)_3$μ-$NH(CH_2PO_3H)_3]$ is synthesized and studied. The crystals are monoclinic, space group $P2_1/c$, $Z = 4$, $a = 9.28230(10)$, $b = 16.0778(2)$, $c = 9.79790(10)$ Å, $\beta = 116.081(2)°$ (CIF file CCDC 1045098). The chrome atom is coordinated at the vertices of the distorted octahedron by three atoms of the water molecules and three O atoms of two tridentate chelate-bridging ligands $NH(CH_2PO_3H)_3$ ($L = H_4NTP^{2-}$). The compound is a linear polymer. The eight-membered cycle Cr–O–P–C–N–C–P–O is closed upon the coordination of ligand L by two oxygen atoms (O(1), O(6)). The O(5) atom is bound to the adjacent chrome atom. The stabilization of the oxidation state of Cr(II) is due to the delocalization of the electron density drawn aside from the metal atom in the PO_3 groups.

DOI: 10.1134/S1070328415100073

INTRODUCTION

The study of the stabilization of unstable oxidation states of transition metals is one of fundamental tasks in chemistry and materials science [1]. The synthesis of complexes is among traditional approaches to the stabilization of elements in oxidation states that are not typical of these elements [2].

The chrome(II) compounds have first been described by Peligot [3]. The synthesis and study of these compounds are impeded by a high reductive ability of both precursors used and products obtained [4]. In air Cr(II) is readily oxidized to Cr(III), while in the absence of air oxygen Cr(II) reduces water with hydrogen evolution [4, 5]. Many chrome(II) complexes were synthesized and studied in spite of technical difficulties [6, 7]. The Cr(II) complexes with alkyl and aryl carboxylate ligands containing clusters $(Cr_2)^{4-}$ and $(Cr_3)^{6-}$ with short Cr–Cr bonds were studied in most detail [8]. The multiplicity from 2 to 4 is ascribed to these bonds [9]. A relative stability of the corresponding compounds in air (up to several hours or even days) is due to the delocalization of valent electrons of chrome in the range of multiple bonds. The chrome(II) complexes with phenyl-phosphates, phenyl-phosphonates, and phenyl-phosphinates were isolated and studied using spectroscopy [10].

Organopolyphosphonic acids form a wide class of chelating agents with different dentate modes and a large stereochemical variety of isolated complexes [11]. Many of these substances showed a high efficiency as corrosion inhibitors [12]. The mechanism of their action is the formation of protective films of coordination compounds with metal ions on the surface of steel and alloys [13]. Chrome is one of the most abundant alloying elements for steels [14], due to which the products of its reactions with organopolyphosphonic acids play an important role in the mechanism of the anticorrosion effect of the latter. In spite of this, Cr(II) complexes with organopolyphosphonic acids are insufficiently studied. For example, the work [7] contains only one reference related to the chrome(II) 1-hydroxyethylidenediphosphonate complexes [15]. The synthesized compounds stable in dry air were isolated and spectroscopically characterized, but their structures were not determined.

Nitrilotris(methylenephosphonic) acid $N(CH_2PO_3)_3H_6$ (**H_6NTP**) is an abundant corrosion inhibitor for steel and a series of other metals [16] and, hence, the study of the structures and properties of chrome(II) coordination compounds with NTP is urgent. The synthesis, crystal structure, and thermal stability of nitrilotris(methylenephosphonato)triaquachrome(II), $[Cr^{II}(H_2O)_3\{$μ-$NH(CH_2PO_3H)_3\}]$ or $[Cr(H_2O)_3$(μ-$H_4NTP)]$ (**I**), are described in this work.

Table 1. Crystallographic characteristics and the experimental and refinement data for structure **I**

Parameter	Value
M	403.08
Crystal system, space group; Z	Monoclinic; $P2_1/c$; 4
a, Å	9.28230(10)
b, Å	16.0778(2)
c, Å	9.79790(10)
β, deg	116.081(2)
V, Å^3	1313.33(3)
ρ_{calcd}, g/cm^3	2.039
Radiation; λ, Å; monochromator	MoK_α; 0.71073; graphite
μ, mm^{-1}	1.299
T, K	293(2)
Sample sizes, mm	0.360 × 0.257 × 0.097
Diffractometer	Xcalibur, Sapphire3, Gemini
Scan type	ω
Absorption correction; T_{min}/T_{max}	[19]; 0.613/0.853
F(000)	824
Measurement θ range, deg	3.433–37.913
Ranges h, k, l	$-15 \le h \le 15$, $-27 \le k \le 27$, $-16 \le l \le 16$
Number of measured/independent reflections (N_1)	43582/6821
R_{int}	0.0231
Number of reflections with $I > 2\sigma(I)$ (N_2)	6294
Refinement method	Full-matrix least-squares method for F^2
Number of refined parameters	245
GOOF	1.073
R_1/wR_2 for N_1	0.0265/0.0644
R_1/wR_2 for N_2	0.0237/0.0632
$\Delta\rho_{min}$ / $\Delta\rho_{max}$, e/Å^3	–0.737/0.704
Programs	SHELX [20], WinGX [21]

EXPERIMENTAL

An aqueous solution of chrome(II) chloride was obtained by the dissolution of powdered electrolytic chrome (>99%) in dilute hydrochloric acid (reagent grade, GOST 3118-77) at 40–60°C in a flask equipped with a stopper with the Bunsen valve. For the better protection of the solution from oxidation, the solution surface was poured with a Nujol layer (GOST 3164-78).

Synthesis of I was carried out in a silicic acid gel [17, 18]. A mixture of a solution (2.5 cm^3) of 70% acetic acid with an aqueous solution containing a solution (5.0 cm^3) of Na_2SiO_3 (density 1.24 g/cm^3) was placed in a U-shaped tube. After the formation of the silicic acid gel, its surface was poured with a Nujol layer to exclude contact with air. A 1 M solution (5 cm^3) of $CrCl_2$ was introduced into one branch of the tube under the Nujol layer using a syringe with a long needle, and another branch was filled with a 1 M solution (5 cm^3) of NTP (doubly recrystallized). Both branches of the tube were closed with stoppers. The branch containing $CrCl_2$ was equipped with the Bunsen valve to remove hydrogen formed. Thus, any contact of the reaction medium with air was completely excluded. After 2 months, light blue (with a greenish shade) transparent monoclinic crystals of complex **I** with the size from 0.1 to 4 mm were formed. After the tube was opened, the reaction mixture containing $CrCl_2$ was oxidized with air oxygen within several seconds to form dark green Cr^{3+} compounds. The crystals of compound **I** turned out to be resistant to air in both the dry and moist state. The product was mechanically separated, washed with water and ethanol, and dried at room temperature.

X-ray diffraction analysis. The crystallographic characteristics and the experimental and refinement parameters for structure **I** are presented in Table 1. The primary fragment of the structure was found by a direct method. Positions of non-hydrogen atoms were

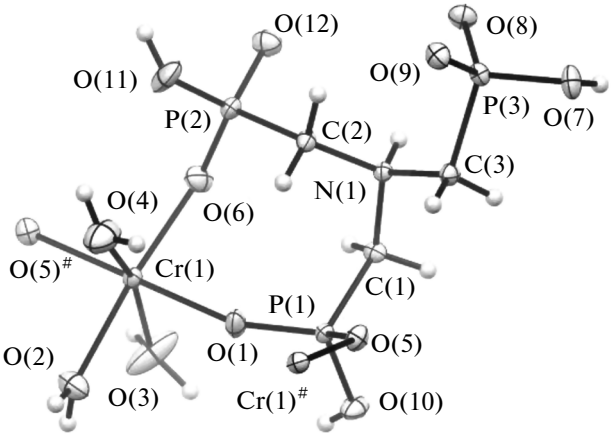

Fig. 1. Fragment of the nitrilotris(methylenephosphonato)triaquachrome(II) structure.

determined from difference electron density syntheses and refined in the anisotropic approximation by least squares for $|F|^2$. Positions of hydrogen atoms were determined from the difference electron density synthesis and refined independently in the isotropic approximation. The results of X-ray diffraction studies of structure **I** were deposited with the Cambridge Crystallographic Data Centre (CIF file CCDC 1045098; deposit@ccdc.cam.ac.uk or http://www.ccdc.cam.ac.uk/data_request/cif).

The electronic absorption spectrum of complex **I** was recorded on an SF-56 spectrophotometer in a range of 190–1100 nm in a quartz cell with an absorption layer thickness of 1 cm. A suspension of compound **I** in Nujol was used.

The IR spectra of compound **I** and its decomposition products were obtained on an FSM-1202 FT-IR spectrometer in a range of 450–5000 cm^{-1}, pressing pellets containing 1 mg of the substance in 250 mg of KBr.

The Raman spectra of crystals **I** were recorded in a range of 470–570 nm on a Centaur U-HR microscope–microspectrometer with laser excitation at a wavelength of 473 nm.

The thermogravimetric analysis of compound **I** in an atmosphere of air and argon was carried out on a Shimadzu DTG-60H automated derivatograph in a temperature range of 30–500°C at a heating rate of 3°C/min.

RESULTS AND DISCUSSION

The fragment of structure **I** is shown in Fig. 1. The interatomic distances and bond angles are given in Table 2. The structural unit of crystal **I** is asymmetric (point symmetry group C_1). Four formula units as a complex of polymer chains parallel to the direction [001] fall onto a unit cell. The packing is caused by the van der Waals interactions and hydrogen bonds.

The molecule of ligand H_4NTP^{2-} in the structure of the complex retains the zwitterionic structure characteristic of free H_6NTP [22]. Each phosphonate group contains two deprotonated oxygen atoms and one protonated oxygen atom, and the nitrogen atom is also protonated and is not involved in coordination with the metal. Two protons of the phosphonate groups of the ligands are substituted by the Cr^{2+} ion with the closure of the eight-membered chelate Cr–O–P–C–N–C–P–O during the formation of complex **I**. The P–O distance for the deprotonated oxygen atoms is 1.4971(7)–1.5162(7) Å, and that for the protonated O atoms ranges from 1.5568(8) to 1.5648(7 Å. The OPC angles for the deprotonated oxygen atoms (107.46(4)°–110.33(5)°) deviate from the ideal tetrahedral angle (109.47°) by no more than 2.01°. For the protonated oxygen atoms, the (H)OPC angles (98.79(4)°–104.65(4)°) are significantly (by 4.82°–10.68°) smaller than the ideal tetrahedral angle, which is explained by the mutual repulsion of the oxygen atoms and a higher angular mobility of the protonated oxygen atom compared to the deprotonated atoms. The repulsion of the deprotonated oxygen atoms also increases the OPO angles between these atoms (to 114.60(5)°–115.55(4)°) compared to the O–P–O(H) angles (106.76(4)°–112.95(5)°). In each phosphonate group, all oxygen atoms are symmetrically nonequivalent. All the three PO_3 groups are also symmetrically nonequivalent: one of them coordinates two chrome atoms (through different oxygen atoms), the second group coordinates one chrome atom, and the third group does not participate in metal coordination.

The structure of CrNTP resembles the earlier studied structures of the protonated nitrilotris(methylenephosphonate) complexes of 3*d* elements [23–25]. The copper(II) nitrilotris(methylenephosphonate) complex [(CuH_4NTP)] (**II**) shows an especially close analogy [26, 27]. It is well known [6, 7] that the coordination compounds of both Cr(II) (d^4) and Cu(II) (d^9) are characterized by the Jahn–Teller effect [28], which manifests itself as a decrease in symmetry of the coordination environment. A comparison of the Cr(II) complexes with the Cu(II) complexes having a similar structure makes it possible to deeper understand the influence of the Jahn–Teller effect on the structures and properties of the coordination compounds.

The chrome(II) atom in structure **I** is coordinated by six oxygen atoms at the vertices of the distorted octahedron (Cr–O 2.0274(7)–2.4119(12) Å, OCrO angles 162.90(4)°–179.03(3)° and 85.79(4)°–101.89(5)°). The average Cr–O distance in structure 2.1681 Å is consistent with the ionic radius of octahedrally coordinated Cr^{2+} in the high-spin state (0.80 Å) [29]. The octahedron is distorted over all three axes (***g***, ***m***, ***p***) (O–Cr_g 2.2743(11) and Å, O–Cr_m 2.1037(8) and 2.1414(8) Å, O–Cr_p 2.0274(7) and 2.0504(6) Å),

Table 2. Interatomic distances (d) and bond angles (ω) in structure **I***

Bond	d, Å	Bond	d, Å	Bond	d, Å
$Cr(1)–O(1)_p$	2.0274(7)	N(1)–C(2)	1.5003(10)	P(1)–O(10H)	1.5648(7)
$Cr(1)–O(2w)_m$	2.1414(8)	N(1)–C(3)	1.5083(10)	P(2)–O(6)	1.5093(8)
$Cr(1)–O(3w)_g$	2.2743(11)	C(1)–P(1)	1.8266(8)	P(2)–O(11H)	1.5568(8)
$Cr(1)–O(4w)_g$	2.4119(12)	C(2)–P(2)	1.8253(8)	P(2)–O(12)	1.4984(8)
$Cr(1)–O(5)^{\#}_p$	2.0504(6)	C(3)–P(3)	1.8331(8)	P(3)–O(7H)	1.5639(7)
$Cr(1)–O(6)_m$	2.1037(8)	P(1)–O(1)	1.4971(7)	P(3)–O(8)	1.5020(7)
N(1)–C(1)	1.5106(10)	P(1)–O(5)	1.5030(7)	P(3)–O(9)	1.5162(7)
Angle	ω, deg	Angle	ω, deg	Angle	ω, deg
O(1)Cr(1)O(2)	87.62(3)	$O(2)Cr(1)O(6)_m$	174.59(3)	O(5)P(1)O(10)	109.29(4)
O(1)Cr(1)O(3)	89.33(4)	$O(3)Cr(1)O(4)_g$	162.90(4)	O(6)P(2)C(2)	110.36(4)
O(1)Cr(1)O(4)	85.79(4)	C(1)N(1)C(2)	114.11(6)	O(11H)P(2)C(2)	98.79(4)
O(1)Cr(1)O(6)	88.84(3)	C(1)N(1)C(3)	110.82(6)	O(12)P(2)C(2)	108.66(4)
O(2)Cr(1)O(3)	81.50(5)	C(2)N(1)C(3)	111.36(6)	O(6)P(2)O(11)	110.33(5)
O(2)Cr(1)O(4)	81.93(5)	N(1)C(1)P(1)	117.77(5)	O(6)P(2)O(12)	114.60(5)
$O(2)Cr(1)O(5)^{\#}$	91.95(3)	N(1)C(2)P(2)	115.18(5)	O(11)P(2)O(12)	112.95(5)
$O(3)Cr(1)O(5)^{\#}$	91.47(4)	N(1)C(3)P(3)	112.66(5)	O(7H)P(3)C(3)	104.65(4)
O(3)Cr(1)O(6)	94.37(5)	O(1)P(1)C(1)	109.92(4)	O(8)P(3)C(3)	107.46(4)
O(4)Cr(1)O(6)	101.89(5)	O(5)P(1)C(1)	109.42(4)	O(9)P(3)C(3)	108.90(4)
$O(4)Cr(1)O(5)^{\#}$	83.12(4)	O(10H) P(1)C(1)	100.62(4)	O(7)P(3)O(8)	112.94(4)
$O(5)^{\#}Cr(1)O(6)$	91.65(3)	O(1)P(1)O(5)	115.28(4)	O(7)P(3)O(9)	106.76(4)
$O(1)Cr(1)O(5)^{\#}_p$	179.03(3)	O(1)P(1)O(10)	111.32(5)	O(8)P(3)O(9)	115.55(4)

* Atom in the symmetrically equivalent position: $^{\#}$ x, $1/2 - y$, $1/2 + z$.

Table 3. Geometric distortions of the Cr(II) coordination octahedron in structure **I**

Octahedron axis	Average length of half-axis (CrO), Å	Difference in half-axes, Å	Deviation of OCrO angle from flat angle (180°), deg	Equivalent thermal parameters of O atoms, Å
Shorter	2.0389(7)	0.0230(13)	0.97(3)	0.01636(11), 0.02142(13)
Medial	2.1226(8)	0.0377(16)	5.41(3)	0.02364(14), 0.02650(15)
Longer	2.3431(12)	0.1376(23)	17.10(4)	0.0395(2), 0.0530(4)

and the ratio of axes of the octahedra is $d_g : d_m : d_p = 1.10 : 1 : 0.96$. According to this, the octahedron has three pairs of vertices: distal vertices lying on axis g and most remote from the center, proximal vertices closest to the center (axis p), and medial vertices occupying an intermediate position. In structure **II**, the average Cu–O distance (2.0966 Å) is also consistent with the ionic radius of copper (0.73 Å) [29] and the ratio of axes of the coordination octahedron of the copper(II) atom in structure **II** ($d_g : d_m : d_p = 1.13 : 1 : 0.96$) is close to the configuration of the environment of chrome(II) in compound **I**. However, the properties of compounds **I** and **II** differ sharply. Copper compound **II** is soluble in water, and its dissolution is accompanied by the hydrolysis of the coordination polymer at the Cu–O bond of the main polymer chain. Chrome complex **I** is insoluble in water and resistant to oxidation in both dry and moist air for at least several months. The stability of structure **I** compared to structure **II** is due to the fact that the Cu–O bonds of the main polymer chain in structure **II** occurs through the oxygen atoms localized in two distal and one medial vertices of the three-axis octahedron. This results in a decrease in the force constant of the Cu–O bonds of the main polymer chain and an easy hydrolysis of compound **II**. In structure **I**, the Cr–O bonds of the main polymer chain occur through two proximal and one medial vertices of the octahedron. The difference in mobilities of the oxygen atoms in the proximal and distal positions can be monitored by the data in Table 3: an increase in

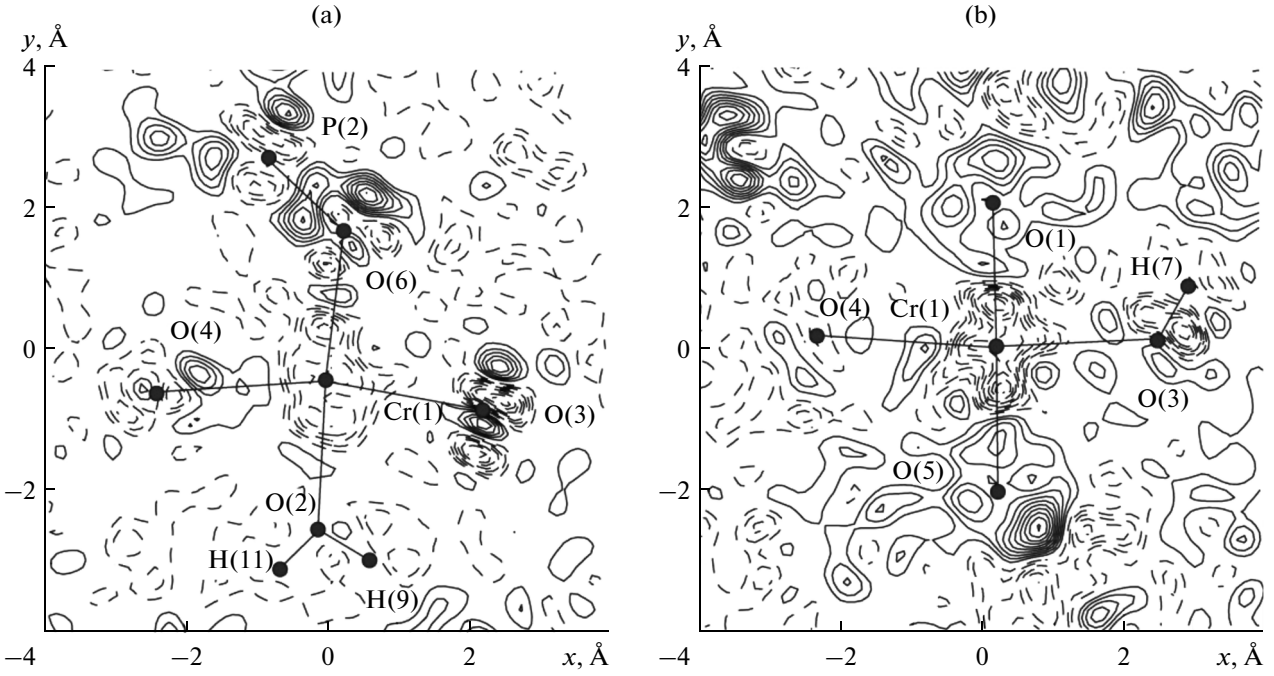

Fig. 2. Difference electron density maps in the coordination environment of Cr^{2+}: in the (a) O(2)O(3)O(6) and (b) O(1)O(3)O(5) planes. The isoline of positive values of the difference in the observed and calculated densities is shown by solid lines and the isoline of the negative values is shown by dashed lines. The increment of the isolines is 0.05 e/A^3.

the Cr–O distance by 0.3 Å, on the average, increases the difference in bond lengths by 6 times, the deviations of the bond angle from the flat angle increase by 17.6 times, and the equivalent thermal parameters increase by 2.45 times. Therefore, the coordination of the chrome(II) atom in the main polymer chain through the proximal vertices of the coordination polyhedron enhances the strength of the corresponding bonds and resistance of complex **I** to hydrolytic and oxidative actions.

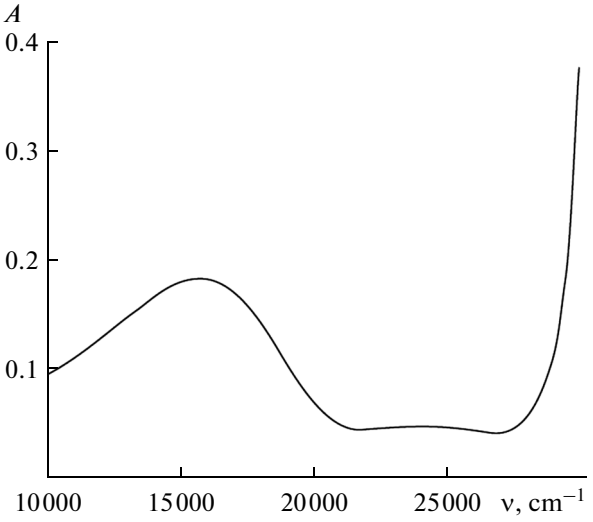

Fig. 3. Electronic absorption spectrum of complex **I** (suspension in Nujol, 0.2 mmol/cm^3).

The difference between the Cr–O(P) and Cr–OH_2 bonds is also seen from the electron density distribution in the coordination environment of the chrome atom (Fig. 2). It is seen that an electron density excess is observed on the oxygen atoms O(1), O(5), and O(6) in the PO_3 groups and on the lines of the Cr(1)–O(1), Cr(1)–O(5), and Cr(1)–O(6) bonds due to the displacement of electrons from the Cr atom. The electron density is also distributed in the P(2)–O(6) bond range. On the contrary, no electron density excess is observed on the O(2), O(3), and O(4) oxygen atoms in the H_2O molecules. It is most likely that the possibility of π-P–O bond delocalization leads to the situation when the PO_3 group behaves as a soft base [30], stabilizing the low oxidation state of chrome [31].

The oxidation state of chrome(II) in compound **I** is confirmed by the electron absorption spectrum (Fig. 3) containing a broad asymmetric band at 11000–20000 cm^{-1} including several *d*–*d* transitions in this range (first of all, $^5B_{1g}$–$^5A_{1g}$ and $^5B_{1g}$–$^5T_{2g}$) split due to the Jahn–Teller effect of asymmetry of the coordination environment, which is characteristic of the Cr(II) complexes [4]. The intense charge-transfer bands lie in a wave number range of 30000 cm^{-1} and higher.

The molecular vibronic spectra of compound **I** (Fig. 4) confirm its structure. The bands 450 ν_{as}(Cr–OH_2), 490 ν_s(Cr–OH_2), 565 ν_{as}(Cr–O(P)), 595

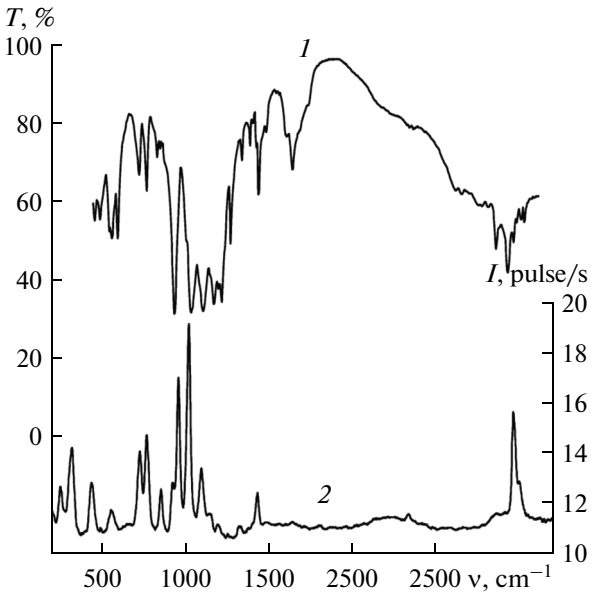

Fig. 4. Molecular vibronic spectra of complex **I**: (*1*) transmission IR spectrum and (*2*) Raman spectrum as functions of wave number ν.

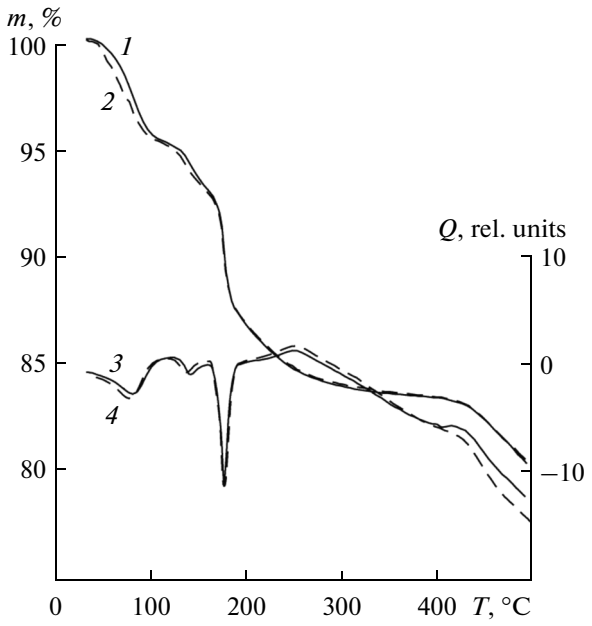

Fig. 5. (*1, 2*) TG and (*3, 4*) TGA curves for complex **I** on heating in (*1, 3*) air and (*2, 4*) argon.

ν_s(Cr–O(P)) cm^{-1} are assigned to vibrations of the coordination sphere of the Cr(II) atom. The presence of these bands in the IR spectrum indicates asymmetry of the coordination polyhedron. No bands of symmetric vibrations are observed in the Raman spectrum. The bands at 725, 770, 930, 960, 1025, 1100, 1170, and 1220 cm^{-1} are attributed to vibrational modes of three symmetrically nonequivalent phosphonate groups, and only some of these lines obey the alternative prohibition rule. The band at 1270 cm^{-1} is assigned to vibrations of the π-P–O bonds. Only the asymmetric mode appears in the Raman spectrum for the methylene groups 1435 $\delta_{as}(CH_2)$, 1485 $\delta_s(CH_2)$, 2960 $\nu_{as}(CH_2)$, and 2980 $\nu_s(CH_2)$ cm^{-1}.

The thermogravimetric study of compound **I** (Fig. 5) also showed substantial differences from the earlier studied copper and zinc complexes [26] in which the removal of three water molecules coordinating the metal atom occurs in three particular steps in a range of 50–150°C. Upon the calcination of compound **I**, one water molecule is removed in a range of 50–100°C. A divergence between changes in the sample weight in air and in an argon atmosphere is observed in the same range. The removal of the second water molecule also occurs in a wide range (125–170°C). The third water molecule (most likely, from the medial vertex of the coordination polyhedron) is eliminated in a range of 170–185°C with a large heat expense. No exotherms are observed for the thermal decomposition of compound **I**, except for the very weak heat evolution upon the elimination of nitrogen (225–275°C). The endothermic destruction and vaporization of the decomposition products of ligand H_4NTP^{2-} occur above 300°C. The IR spectrum of the solid decomposition products exhibit characteristic bands of chrome(III) metaphosphate [32]: 480, 580, 770, 900, 940, 1120, and 1230 cm^{-1}.

The insolubility in water and the oxidative and thermal stability of complex **I** make it possible to consider this compound as a promising ingredient of anticorrosion protective coatings on the surface of chromium steels for corrosion inhibition by H_6NTP and its derivatives.

ACKNOWLEDGMENTS

This work was carried out in the framework of task no. 2014/134 of the fulfillment of state works in the sphere of scientific activities in terms of the basic part of the state task, project code 2312.

REFERENCES

1. Kleinberg, J., *Unfamiliar Oxidation States and Their Stabilization*, Lawrence: Univ. of Kansas, 1950, p. 132.
2. Kiselev, Yu.M. and Tret'yakov, Yu.D., *Usp. Khim.*, 1999, vol. 68, no. 5, p. 401.
3. Peligot, E.-M., *C.R. Acad. Sci.*, 1844, vol. 19, p. 609.
4. Lever, A.B.P., *Inorganic Electronic Spectroscopy*, Amsterdam: Elsevier, 1987, vol. 2.
5. Cotton, F.A. and Wilkinson, J., *Advanced Inorganic Chemistry*, New York: Wiley, 1966, vol. 3.
6. *Comprehensive Coordination Chemistry*, Wilkinson, J., Ed., Oxford: Pergamon, 1987, vol. 3.
7. *Comprehensive Coordination Chemistry II*, McCleverty, J.A., Meyer T.J., and Wedd, A.G., Eds., Amsterdam: Elsevier, 2003, vol. 4.

8. Cotton, F.A., Hillard, E.A., Murillo, C.A., and Zhou, H.C., *J. Am. Chem. Soc.*, 2000, vol. 122, p. 416.
9. Clerac, R., Cotton, F.A., Daniels, L.M., et al., *Inorg. Chem.*, 2000, vol. 39, p. 748.
10. Larkworthy, L.F. and Salib, K.A.R., *Transition Met. Chem.*, 1986, vol. 11, p. 121.
11. Dyatlova, N.M., Temkina, V.Ya., and Popov, K.I., *Kompleksony i kompleksonaty metallov* (Complexones and Metal Complexonates), Moscow: Khimiya, 1988.
12. Kuznetsov, Yu.I., *Usp. Khim.*, 2004, vol. 73, no. 1, p. 79.
13. Naimushina, E.A., Chausov, F.F., Kazantseva, I.S., and Shabanova, I.N., *Izv. Akad. Nauk, Ser. Fiz.*, 2013, vol. 77, no. 3, p. 362.
14. Rzhevskaya, S.V., *Materialovedenie* (Material Science), Moscow: MGGU, 2003.
15. Popova, T.V., Smotrina, T.V., Denisova, O.N., and Aksenova, N.V., *Russ. J. Coord. Chem.*, 2001, vol. 27, no. 1, p. 38.
16. Naimushina, E.A., Chausov, F.F., Shabanova, I.N., and Kazantseva, I.S., *Izv. Akad. Nauk, Ser. Fiz.*, 2014, vol. 78, no. 4, p. 436.
17. Henisch, H.K., *Crystal Growth in Gels*, Pennsylvania State University, 1970.
18. Petrov, T.G., Treivus, E.B., Punin, Yu.O., and Kasatkin, A.P., *Vyrashchivanie kristallov iz rastvorov* (Growing Crystals from Solutions), Leningrad: Nedra, 1983.
19. *CrysAlisPro. Version 1.171.37.35*, Yarnton (Oxfordshire): Agilent Technologies, 2014.
20. Sheldrick, G.M., *Acta Crystallogr., Sect. A: Found. Crystallogr.,* 2008, vol. 64, p. 112.
21. Farrugia, L.J., *J. Appl. Crystallogr.*, 1999, vol. 32, p. 837.
22. Daly, J.J. and Wheatley, P.J., *J. Chem. Soc. A*, 1967, p. 212.
23. Sharma, C.V.K. and Clearfield, A., *J. Am. Chem. Soc.,* 2001, vol. 123, p. 2885.
24. Cabeza, A., Ouyang, X., Sharma, C.V.K., et al., *Inorg. Chem.*, 2002, vol. 41, p. 2325.
25. Demadis, K.D., Katarachia, S.D., and Koutmos, M., *Inorg. Chem. Comm.,* 2005, no. 8, p. 254.
26. Chausov, F.F., Zakirova, R.M., Somov, N.V., et al., *Zh. Prikl. Khim.*, 2014, vol. 87, no. 8, p. 1046.
27. Somov, N.V. and Chausov, F.F., *Kristallografiya*, 2015, vol. 60, no. 2, p. 233.
28. Bersuker, I.B., *The Jahn-Teller Effect and Vibronic Interactions in Modern Chemistry*, Cham: Springer, 2013.
29. Shannon, R.D., *Acta Crystallogr., Sect. A: Cryst. Phys., Diffr., Theor. Gen. Crystallogr.*, 1976, vol. 32, p. 751.
30. Pirson, R.D., *Usp. Khim.*, 1971, vol. 40, no. 7, p. 1259.
31. Anorganikum Kolditz, L., Ed., Berlin: VEB Deutscher Verlar der Wissenschaften, 1984.
32. Fuks, H., Kaczmarek, S.M., and Bosacka, M., *Rev. Adv. Mater. Sci.*, 2010, vol. 23, p. 57.

Translated by E. Yablonskaya